

The yield and thermoelastic properties of oriented poly(methyl methacrylate)

P. A. Botto, R. A. Duckett and I. M. Ward

*Department of Physics, University of Leeds, Leeds LS2 9JT, UK
(Received 21 May 1986; revised 2 September 1986)*

Oriented sheets of poly(methyl methacrylate) were prepared by drawing to different draw ratios at a range of temperatures near the glass transition temperature. The degree of molecular orientation in these materials was characterized by measuring birefringence, and specimens prepared for measurements of tensile yield stress and shrinkage stress at elevated temperature. The shrinkage stress measurements were carried out by holding specimens at constant length above the glass transition temperature and determining the resulting stress as a function of time. The peak value of stress was found to be a function of birefringence only, independent of draw ratio or draw temperature. The function was linear for a substantial range of birefringence. A further series of specimens was used to measure the tensile yield stress (in the orientation direction) as a function of temperature and strain rate. At each testing temperature it was found that the yield stress correlated uniquely with the birefringence. These results for shrinkage stress and yield stress can both be interpreted through the concept of a frozen-in molecular network, and a semi-quantitative relationship proposed which relates to the anisotropy of the yield stress to the frozen-in network stress. This provides a molecular explanation for the Bauschinger effect observed in oriented polymers.

(Keywords: yield; oriented; PMMA; shrinkage force; birefringence)

INTRODUCTION

This paper attempts to establish a possible connection between two aspects of deformation in polymers: the yield behaviour of oriented polymers, and the development of molecular orientation during drawing. In particular we will examine the evidence which suggests that the presence of a molecular network provides the key to establishing the connection which we believe to exist. To reduce the complexity of the problem we have chosen to study an amorphous polymer, poly(methylmethacrylate) (PMMA), so that there are no effects of crystallization and morphology.

It is now well established that whereas the yield stress in tension of an oriented polymer (parallel to the draw direction) increases with increasing draw ratio, the yield stress in compression remains approximately constant, or even slightly decreases¹. It is intuitively reasonable that this difference arises because in tension the applied stress acts to extend further already extended chains, whereas in compression the stress acts to compress the extended structure. The possibilities of either or both of chain scission and pulling out of entanglements arises in tension, but buckling of extended chains seems more probable in compression. This inequality between the tensile and compressive yield stresses has been described as evidence for the existence of a Bauschinger effect², and has been discussed in terms of a molecular network³. Tensile yield involves further extension of the network, which will be a difficult process and hence require a higher stress than compressive yield, which involves collapse of the network.

The development of molecular orientation in a glassy amorphous polymer on drawing, has also been extensively studied, often by measuring the optical anisotropy or birefringence, and various deformation schemes have been proposed¹. One of the simplest schemes, often called the 'pseudo-affine' model, considers that there is independent orientation of individual anisotropic elements each with uniaxial symmetry⁴. The unique axes of the units are considered to rotate as lines marked in the macroscopic polymer, which deforms at essentially constant volume. The 'pseudo-affine' deformation scheme has been shown to describe the development of molecular orientation in cold drawing of polyethylene terephthalate (PET) to a very good approximation⁵.

A more self consistent scheme (known as the 'affine model') was proposed for rubbers (i.e., above the glass transition temperature T_g) in which the random anisotropic links are connected together to form chains which only interact at well defined junction points⁶. According to this scheme, as deformation progresses each chain becomes more elongated whilst rotating towards the draw direction. At all stages each chain (or strictly each segment of chain between junction points) attempts to maximize its entropy by disorienting the elements or random links, subject only to the constraints imposed by the end-to-end vectors (between junction points). These vectors are assumed to deform as would macroscopic lines drawn in the material. In a polymer such as PMMA the chains are joined only by physical entanglements, rather than by precise and permanent chemical cross-

links. Raha and Bowden⁷ showed that the development of birefringence with strain in PMMA deformed in the glassy state could be described by this scheme if the number of chains per unit volume was allowed to decrease with deformation because of pulling out of entanglements.

In spite of the apparent success in PET of the pseudo-affine model of independently rotating elements, firm evidence for the existence of an oriented molecular network has also been obtained for this polymer when drawn above T_g . If oriented PET samples are maintained at constant length at a temperature just above the glass transition temperature T_g a shrinkage force develops, relating precisely to the birefringence in a manner predicted for an extended rubber-like network^{8,9}. Moreover, it appears that the limiting extensibility observed in cold drawing (the so-called 'natural draw ratio') relates to the limiting extensibility of a molecular network^{5,10,11}.

Kahar, Duckett and Ward¹² have shown that the peak shrinkage stresses observed for hydrostatically extruded PMMA also correlated uniquely with birefringence. This result confirmed the proposal of Raha and Bowden⁷ that orientation involves the deformation of a network, but did not throw much further light on their ideas of breakdown of network junction points with increasing draw ratio.

In this paper we will develop two themes, relating orientation both to network deformation and to the inequality of the yield stress in tension and compression. It is of particular interest to explore the possibility that the entropic stress of the molecular network can be released either by increasing the temperature above T_g or by the input of sufficient mechanical work (up to the yield point) so giving a quantitative explanation of the Bauschinger effect.

EXPERIMENTAL

The material used throughout was commercial grade ICI 'Perspex' sheet of thickness 1.5 mm. Dumbbell specimens were milled to shape using a half-inch radius cutter, polished with silicon carbide paper and then 'Perspex Polish'.

Two main series of experiments were conducted to investigate the development of birefringence, in both cases drawing at a constant displacement rate corresponding to an initial nominal strain-rate of $1.7 \times 10^{-2} \text{ s}^{-1}$. In the first series drawing was effected at 90°C over a range of draw ratios $2.2 < \lambda < 3.0$, this range defined by non-uniformity of strain at the lower end and by fracture at the high end. Draw-ratios were calculated by measuring the cross-sectional area of the drawn and undrawn specimens using a micrometer, making the assumption of constant volume. In the second series the temperature was 135°C (i.e. above the T_g of 105°C) and draw ratios from 1 to 4.5 were obtained. By these means specimens with birefringence values from 0 to -15×10^{-4} were obtained. Birefringences were measured in a polarizing microscope using an Eyringhaus rotating calcite-plate compensator.

Yield stresses in tension parallel to the initial draw direction were measured at a strain-rate of $1.7 \times 10^{-2} \text{ s}^{-1}$ over the full range of birefringence at -30°C , -15°C , 0°C , 15.5°C , 30°C , 40°C , 50°C , 60°C , 70°C , 80°C and

90°C . Note that measurements on the isotropic sheets could only be made above 40°C because premature fracture through crazing occurred at lower temperatures. Even low levels of orientation appear to suppress craze formation and allow ductile deformation down to -30°C in oriented materials. Tests at elevated temperatures were only possible on specimens which had been stabilized by annealing at constant length at the test temperature for two hours. This procedure ensured that the specimens were then subsequently stable against free annealing at any lower temperature for a period of 1 hour with only an additional 1% loss in birefringence. Highly oriented specimens did not show a load drop at yield. Following a series of trials involving loading the specimen to a series of different strains and then unloading, it was noted that the permanent strain and residual birefringence started to increase more steeply at round 5–7%. This indicated a yield point which corresponded almost exactly to a '2% offset yield criterion'¹³ which was then used for convenience in all subsequent tests.

A further series of yield stress measurements was completed to measure the strain-rate sensitivity of both isotropic material, at temperatures 30°C , 70°C and 95°C and of oriented material (with birefringence of -15×10^{-4}) at 30°C .

Samples for shrinkage force measurement were cut from specimens previously deformed in tension to dimensions approximately $60 \times 1 \times 0.5 \text{ mm}$. These were held at constant length and then immersed in a temperature controlled oil bath maintained at 120°C : the force generated was measured by a strain-gauge dynamometer and recorded on a chart recorder. A few shrinkage force measurements were also made at other temperatures in the range 110°C to 200°C .

RESULTS AND DISCUSSION

Drawing studies

The development of birefringence with draw ratio on drawing at 90°C is shown in Figure 1. Also shown in the Figure are two curves calculated from the 'pseudo-affine' model⁵ according to equation (1).

$$\Delta n = \frac{\Delta n_{\max}}{2} \left[\frac{3}{(1 - \lambda^{-3})} - \frac{3\lambda^{-3/2} \cos^{-1}(\lambda^{-3/2})}{(1 - \lambda^{-3})^{3/2}} - 1 \right] \quad (1)$$

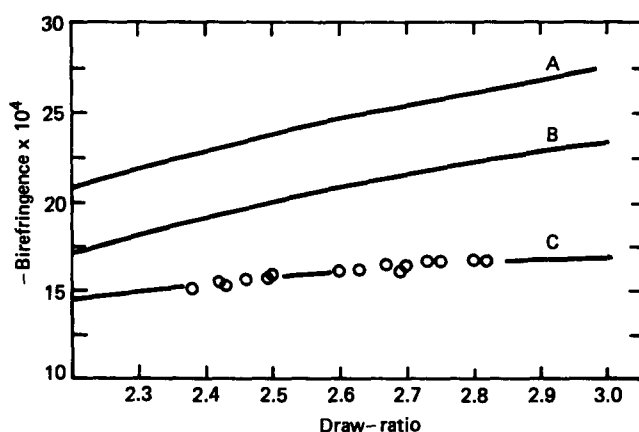


Figure 1 Birefringence vs. draw ratio for samples drawn at 90°C . Curves (A) equation (1) with $\Delta n_{\max} = -43 \times 10^{-4}$. (B) equation (1) with $\Delta n_{\max} = -35.5 \times 10^{-4}$. (C) equation (3) with data from Table I

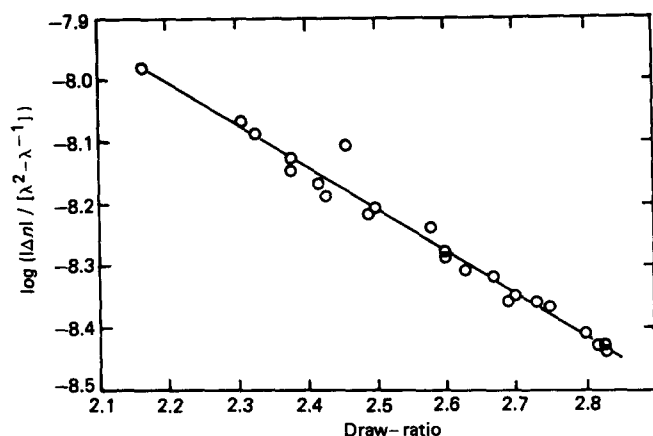


Figure 2 $\log(\Delta n/(\lambda^2 - \lambda^{-1}))$ vs. λ for samples drawn at 90°C

In this equation λ represents the draw ratio and Δn_{\max} the maximum birefringence expected for full alignment. There is considerable uncertainty as to the correct value for the theoretical maximum birefringence for PMMA because a large contribution comes from the ester side groups, and its magnitude depends on the conformation and motion of this group which are both unclear. Values of -43×10^{-4} and -35.5×10^{-4} have both been proposed for Δn_{\max} based on experimental measurements of the second moment of the orientation distribution function using broad-line n.m.r.¹⁴ and laser-Raman spectroscopy¹⁵ respectively and the two curves (A) and (B) drawn correspond to these two values. It is clear that no choice of Δn_{\max} will provide a good fit to these data using the pseudo-affine model.

The affine model proposed for rubbers is also inappropriate because it predicts the opposite curvature to that observed experimentally. However the modification proposed by Raha and Bowden⁷ in which the number of chains per unit volume N decreases exponentially with increasing strain is capable of describing these data accurately. According to this scheme the birefringence evolves with strain according to equation (2).

$$\Delta n = CN_0(\alpha_1 - \alpha_2)(\lambda^2 - \lambda^{-1})\exp(-k(\lambda - 1)) \quad (2)$$

where

$$C = \frac{2\pi(\bar{n}^2 + 2)^2}{45n}$$

and \bar{n} is the mean refractive index, C has the value 1.645 for PMMA, $(\alpha_1 - \alpha_2)$ is the difference in principal polarizabilities of the random link, N_0 is the number of chains/unit volume at zero strain and k determines the rate of breakdown of the network. Figure 2 shows the data plotted in the form of $\log(\Delta n/(\lambda^2 - \lambda^{-1}))$ vs. λ , and reveals an acceptable straight line fit as predicted by equation (2). Although equation (2) is adequate to fit the data from samples drawn below the glass transition it provides only a very poor fit to the data covering a wider range of draw-ratios from drawing at 135°C. Equation (2) is clearly unsatisfactory in principle for fitting data at large strains since it predicts the birefringence with decrease to zero.

A simple extension of this Raha and Bowden model is

therefore proposed which can describe both sets of data (high and low temperature) and avoids the difficulty at high strains referred to above. This is a two network model in which it is considered that there is a permanent network with N_p chains/unit volume in addition to a temporary network with N_t chains per unit volume in the unstrained state which breaks down on deformation.

$$\Delta n = C(N_p + N_t \exp(-k(\lambda - 1)))(\alpha_1 - \alpha_2)(\lambda^2 - \lambda^{-1}) \quad (3)$$

This modification described by equation (3) also provides an excellent fit to the data at 90°C as shown by curve (C) in Figure 1 and furthermore provides an excellent fit to the data at 135°C as shown in Figure 3. The addition of a permanent network term removes the difficulty inherent in equation (2) of the birefringence tending to zero as the draw ratio tends to infinity.

Values for the fitting parameters calculated assuming $(\alpha_1 - \alpha_2) = -10^{-30} \text{ m}^3$ are shown in Table 1. It is to be noted that N_t decreases with temperature whereas N_p is substantially constant. This result is consistent with the view that there are two types of junction points, firstly there are the temporary associations resulting from dipolar interactions as speculated by Raha and Bowden⁷, secondly more permanent entanglements, probably associated with molecules in the high molecular weight tail of the molecular weight distribution.

It is acknowledged that the addition of a permanent network term N_p is not strictly necessary to fit the data from samples drawn at 90°C—the term $N_p + N_t \exp(-k(\lambda - 1))$ differs from $N_0 \exp(-k'(\lambda - 1))$ by less than 2% over the limited range of draw ratios accessible using optimized values of the parameters. Its inclusion is justified by seeking consistency of representation over the range of temperatures in view of the need to include such a term to fit the 130°C data.

Yield stresses

The most important feature of the results presented in Figures 4 and 5, true for all test temperatures, is that the

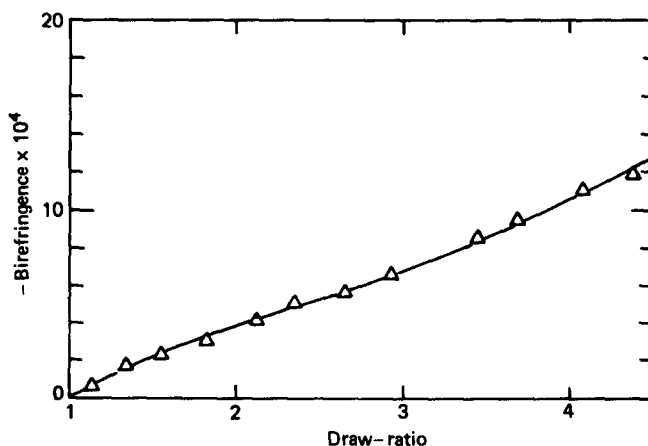


Figure 3 Birefringence vs. draw ratio for samples drawn at 135°C. Curve drawn from equation (3) with data from Table 1

Table 1 Parameters used to describe birefringence data using equation (3)

T (°C)	$N_p \times 10^{-26}$ (m^{-3})	$N_t \times 10^{-26}$ (m^{-3})	k
90	0.38	4.7	0.89
135	0.31	0.63	0.61

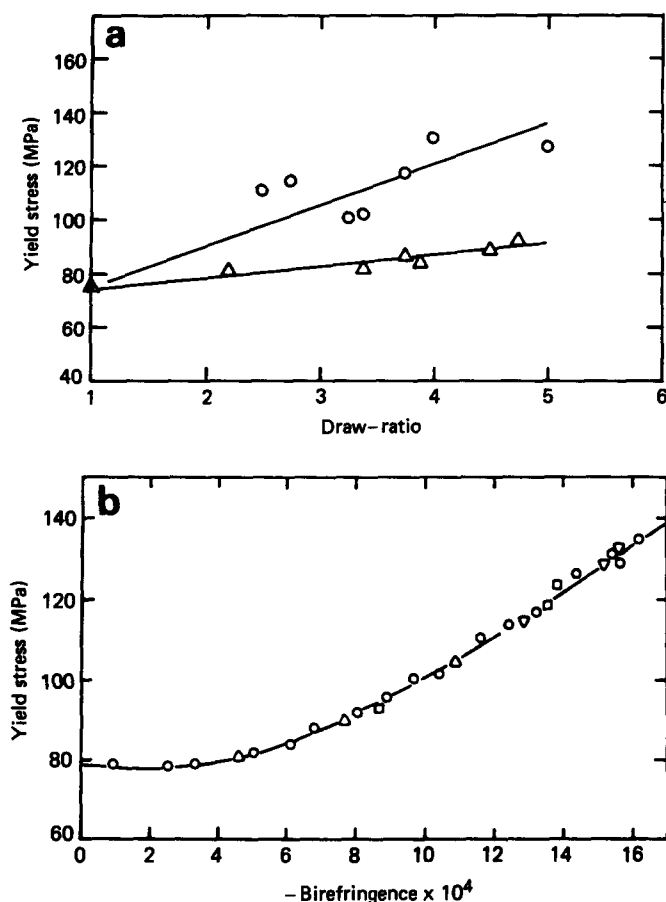


Figure 4 (a) Yield stress data at 30°C vs. λ showing data from samples drawn at 110°C, (○) and 120°C, (△). (b) Yield stress data at 30°C vs. birefringence for samples with different thermal histories: (○), as drawn at different temperatures; (□), annealed at constant length; (△), free annealed; (▽), aged at room temperature

yield stress is a unique function of the birefringence at any test temperature and strain-rate, independent of either draw-ratio or draw temperature. Moreover it is possible to take specimens drawn to a high birefringence, anneal them to give partial recovery, and to find that their yield stress is then identical to that of a specimen drawn directly to the final birefringence.

Measurements were also made of the temperature and strain-rate dependence of the yield stress. For isotropic material the results confirmed quantitatively the findings of previous workers^{16,17}. These previous workers showed that at low temperatures yield is controlled by at least two thermally activated processes which can be considered to act in parallel. The yield stress σ_y is then given by

$$\sigma_y = (\Delta U_\alpha / V_\alpha) + (kT / V_\alpha) \ln(\dot{\epsilon} / \dot{\epsilon}_\alpha) + (kT / V_\beta \sinh^{-1}[(\dot{\epsilon} / 2\dot{\epsilon}_\beta) \exp(\Delta U_\alpha / kT)]) \quad (4)$$

where the two activated processes are denoted by the subscripts α and β respectively. At high temperatures (i.e. above 50°C) the α process predominates and this has a comparatively low strain rate dependence, which justifies the use of the approximation $\sinh x \approx \frac{1}{2} \exp x$. The contribution of the β process, which is identified with the β -relaxation of PMMA is negligible at these temperatures and equation (4) then reduces to

$$\sigma_y = (\Delta U_\alpha / V_\alpha) + (kT / V_\alpha) \ln(\dot{\epsilon} / \dot{\epsilon}_\alpha) \quad (5)$$

and the values obtained for the activation energy and activation volume correspond to the α -process.

At low temperatures and high strain rates, on the other hand, the β -process is also important, and the approximation $\sinh x = \frac{1}{2} \exp x$ can now be applied to this process also, so that

$$\sigma_y = (\Delta U_{app} / V_{app}) + (kT / V_{app}) \ln(\dot{\epsilon} / \dot{\epsilon}_{app})$$

where

$$\frac{1}{V_{app}} = \frac{1}{V_\alpha} + \frac{1}{V_\beta}$$

and

$$\Delta U_{app} = \frac{V_\beta \Delta U_\alpha + V_\alpha \Delta U_\beta}{V_\alpha + V_\beta}$$

The values of V_α , ΔU_α and V_{app} , ΔU_{app} are given in Table 2. The value of ΔU_α of 106 kcal mol⁻¹ has been obtained on the basis that the activation volume is independent of temperature and is consistent with previous work. Qualitatively the results for the drawn materials are similar, except that the temperature and strain rate dependences in the low temperature region become increasingly high for high birefringence. At high

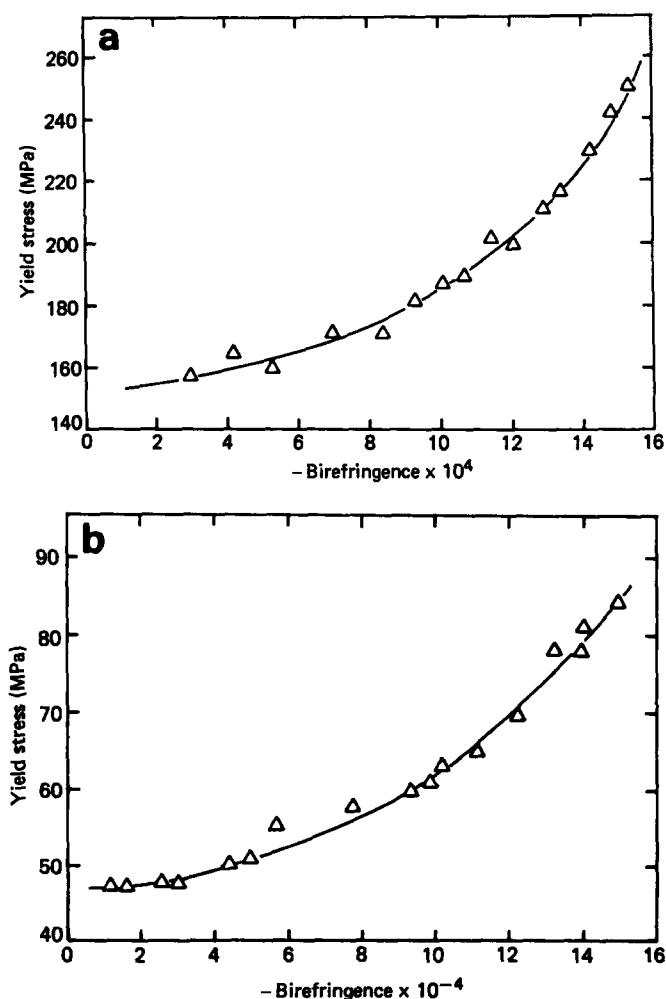
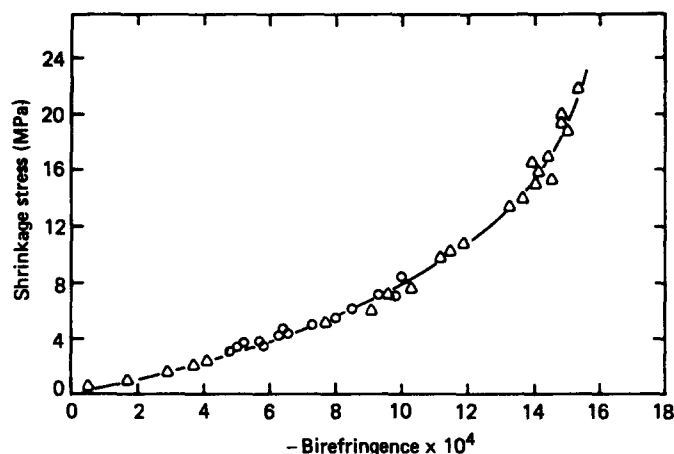


Figure 5 (a) Yield stress data at -30°C vs. birefringence. (b) Yield stress data at 60°C vs. birefringence

Table 2 Effective activation parameters for isotropic and oriented PMMA

Isotropic	ΔU_{eff} (kcal mol ⁻¹)	V_{eff} (Å ³)
$T = 95^\circ\text{C}$	105.7 ± 10.6	1880 ± 100
70°C	51.7 ± 9.3	1570 ± 140
30°C	56.0 ± 10.4	1120 ± 125
Oriented $T = 30^\circ\text{C}$	40.4 ± 6.9	495 ± 40

**Figure 6** Shrinkage stress vs. birefringence, including data (○) from samples produced by hydrostatic extrusion, ref. 12

temperatures the temperature and strain-rate dependences of the yield stress are almost undistinguishable for all values of birefringence, although the absolute values (of the yield stress) continue to increase with increasing birefringence.

Shrinkage forces

In all cases the shrinkage force was observed to increase quickly to a maximum value before decaying more slowly. As in previous work on hydrostatically extruded PMMA¹², the peak value, divided by the current cross-sectional area, correlated closely with the birefringence. Samples of complicated thermo-mechanical history were also studied and in all cases the peak stress was found to correlate closely with the final birefringence. However the drawn specimens studied here extend the range of birefringence previously available by 50%, and it is clear that the relationship is non-linear at high birefringences although the results overlap at low birefringence (see Figure 6).

In an attempt to confirm that the shrinkage force measurement is characterizing the molecular network frozen in when the drawn specimen is unloaded and quenched to below T_g a series of specimens was drawn at 135°C , and the drawing process was interrupted at different strains to measure the birefringence and the cross-section area. From the load just before interruption it was then possible to calculate the true drawing stress. Figure 7 shows a plot of these drawing stresses vs. the birefringence to compare directly with the previous shrinkage stress data. The figure shows clearly that the shrinkage stress above T_g is exactly equal to the drawing stress at each value of birefringence.

GENERAL DISCUSSION

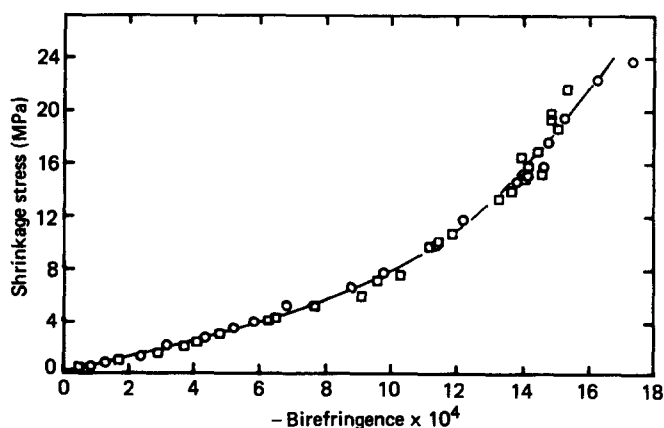
Orientation mechanisms

Neither the pseudo-affine model nor the affine rubber model seem adequate to describe the development of birefringence with deformation. From the viewpoint of curve fitting equation (3) representing the 'two network model', is excellent. On this scheme the majority of junction points are temporary, breaking down progressively with deformation; a minority of junction points are more permanent, and these are perhaps entanglements of the longer chains. It must be pointed out that for deformation at low temperatures the number of chains per unit estimated on the basis of this model is found to be rather high, implying chains which are probably rather too short for reliable use of Gaussian statistics⁶. Although this is less of a problem with data from drawing at 135°C it does seem that a satisfactory understanding of the deformation mechanisms may have to wait until further reliable orientation function averages, \bar{P}_2 and \bar{P}_4 are available from molecular spectroscopy^{14,15}.

The entropic origin of the Bauschinger effect

Two key results here are of remarkable simplicity. First, both the yield stress (at any fixed temperature and strain-rate) and the shrinkage stress are uniquely determined by the birefringence, independent of any details of the thermomechanical history. Secondly, the shrinkage stress has been shown to be exactly equal to the drawing stress for samples drawn at 135°C . This confirms that the network can be considered to be 'locked'- or 'frozen'-in to the strained configuration on cooling below T_g . Raising the temperature above T_g releases this frozen-in stress, which can then cause recovery of dimensions in an unconstrained sample or the build up of a shrinkage stress in a sample held at constant length.

A simple model for the tensile yield behaviour of oriented PMMA can be proposed by assuming that the frozen-in network stress acts in parallel with the viscous stress described by the activated rate processes of equation (4) (i.e. all elements experience the same strain so that the stresses of the elastic and viscous elements are additive). This approach is very similar to that proposed by Haward and Thackray¹⁸. For quasistatic deformation above T_g (e.g. at 135°C) the viscosity term is so low that

**Figure 7** Comparison of shrinkage stress (□) and drawing stress (○) (at 135°C) for different values of birefringence

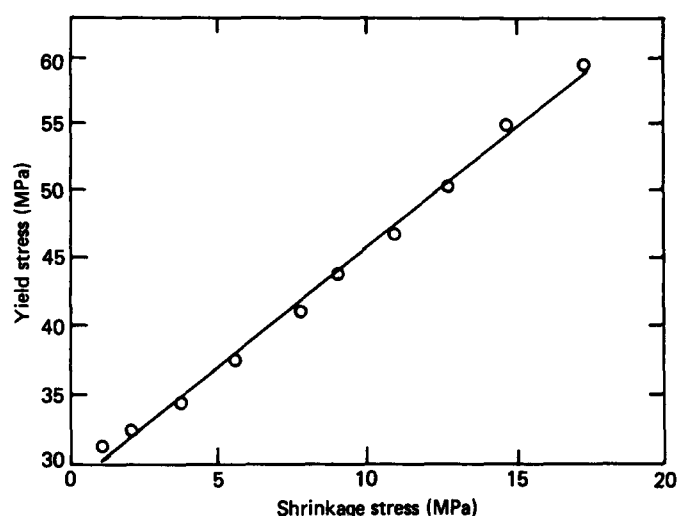


Figure 8 Typical plot of yield stress (at 90°C in this case) vs. shrinkage stress for samples of different birefringence

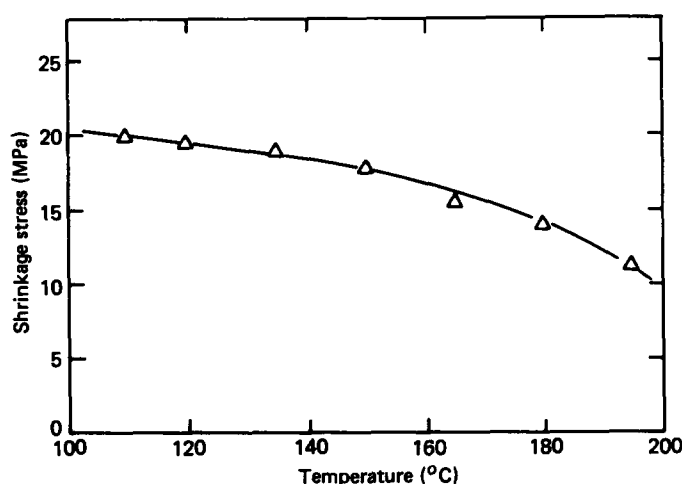


Figure 9 Shrinkage stress vs. shrinkage temperature for birefringence = -14.75×10^{-4}

the mechanics are dominated by the elastic properties of the network. Deformation below T_g involves a contribution from the dashpot so introducing a strain-rate dependence into the response.

According to this simple model the stress-strain behaviour can be described by equation (6)

$$\sigma_y(\epsilon, \dot{\epsilon}, T) = \sigma_{\text{net}}(\epsilon, T) + \sigma_{\text{visc}}(\epsilon, \dot{\epsilon}, T) \quad (6)$$

where $\sigma_{\text{visc}}(\epsilon, \dot{\epsilon}, T)$ is the viscous stress term, and we have allowed for the dependence of this on strain ϵ as well as strain rate and temperature, following results for other oriented polymers¹⁹. $\sigma_{\text{net}}(\epsilon, T)$ represents the dependence of the network stress on strain and temperature of deformation. Figure 6 suggests that this can be represented by the shrinkage stress which is a unique function of the birefringence.

If the viscous term were not dependent on strain there

would be a straight-line relationship of unit slope between the yield stress and the shrinkage stress for results obtained at constant temperature and strain-rate. Figure 8 is typical of such a plot and relates to yield at 90°C. There is clearly an excellent linear correlation between the yield stress σ_y and the shrinkage stresses σ_{net} in this case (and at all other temperatures) but here the slope is 1.87 not 1.0. In fact, inspection of all the data suggests that they can be represented as follows:

$$\sigma_y(\Delta n, \dot{\epsilon}, T) = f(T)\sigma_{\text{net}}(\Delta n) + \sigma_{\text{visc}}(\Delta n, \dot{\epsilon}, T) \quad (7)$$

where $1 < f(T) < 3.5$ ($f = 3.5$ for $T = 30^\circ\text{C}$). $f(T)$ tends to unity as T approaches T_g and the term σ_{visc} becomes very small. It is most important that the birefringence Δn rather than plastic strain ϵ *per se*, appears to be the decisive parameter throughout this equation.

There are several possible reasons why the slope would not be unity below T_g .

(a) The network term is temperature dependent, decreasing with increasing temperature. This possibility has been confirmed for temperatures above T_g by direct measurements of the changing shrinkage force at different temperatures, as shown in Figure 9.

(b) The activation volume for the viscous process decreases with increasing birefringence, similar to the case of polyethylene, extensively documented elsewhere¹⁹.

A more satisfactory quantitative interpretation of these results could probably be obtained by determining the tensile and compressive yield stress over a range of values of birefringence, and covering a wide range of temperatures and strain rates. From the present data it can only be concluded that there is strong qualitative evidence for a substantial contribution to the measured tensile yield stress from the frozen-in network stress.

REFERENCES

- 1 Duckett, R. A. *Int. Metal. Rev.* 1983, **28**, 158
- 2 Brown, N., Duckett, R. A. and Ward, I. M. *Phil. Mag.* 1968, **18**, 483
- 3 Bridle, C., Buckley, A. and Scanlan, J. J. *Mater. Sci.* 1968, **3**, 622
- 4 Ward, I. M. *Proc. Phys. Soc.* 1962, **80**, 1176
- 5 Foot, J. S. and Ward, I. M. *J. Mater. Sci.* 1975, **10**, 955
- 6 Treloar, L. R. G. *Trans. Faraday Soc.* 1954, **50**, 881
- 7 Raha, S. and Bowden, P. B. *Polymer* 1972, **13**, 175
- 8 Pinnock, P. R. and Ward, I. M. *Trans. Faraday Soc.* 1966, **62**, 1308
- 9 Rietsch, F., Duckett, R. A. and Ward, I. M. *Polymer* 1979, **20**, 1133
- 10 Allison, S. W., Pinnock, P. R. and Ward, I. M. *Polymer* 1966, **7**, 66
- 11 Engelaere, J. C., Cavrot, J. P. and Rietsch, F. *Polymer* 1982, **23**, 766
- 12 Kahar, N., Duckett, R. A. and Ward, I. M. *Polymer* 1978, **19**, 136
- 13 Dieter, G. E. 'Mechanical Metallurgy', 2nd Edn., McGraw-Hill, New York, pp. 9 & 10, 1976
- 14 Kashiwagi, M., Folkes, M. J. and Ward, I. M. *Polymer* 1971, **12**, 697
- 15 Purvis, J. and Bower, D. I. *Polymer* 1974, **15**, 645
- 16 Roetling, J. A. *Polymer* 1965, **6**, 311
- 17 Bauwens-Crowet, C. *J. Mater. Sci.* 1973, **8**, 968
- 18 Haward, R. N. and Thackray, G. *Proc. Roy. Soc., London* 1968, **A302**, 453
- 19 Coates, P. D. and Ward, I. M. *J. Mater. Sci.* 1978, **13**, 1957